

# Hot-carrier multi-junction solar cells: A synergistic approach

Cite as: Appl. Phys. Lett. **120**, 213901 (2022); doi: [10.1063/5.0073274](https://doi.org/10.1063/5.0073274)

Submitted: 29 September 2021 · Accepted: 20 December 2021 ·

Published Online: 24 May 2022



View Online



Export Citation



CrossMark

Maxime Giteau,<sup>1,4,a)</sup>  Samy Almosni,<sup>2,4</sup>  and Jean-François Guillemoles<sup>3,4,a)</sup> 

## AFFILIATIONS

<sup>1</sup>Research Center for Advanced Science and Technology (RCAST), The University of Tokyo, Komaba 4-6-1, Meguro-ku, Tokyo 153-8904, Japan

<sup>2</sup>Saule Technologies, Wroclaw Technology Park, 11 Dunska, 54-130 Wroclaw, Poland

<sup>3</sup>CNRS, Institut Photovoltaïque d'Ile de France (IPVF), UMR 9006, 18 Boulevard Thomas Gobert, 91120 Palaiseau, France

<sup>4</sup>NextPV, LIA RCAST-CNRS, The University of Tokyo, Komaba 4-6-1, Meguro-ku, Tokyo 153-8904, Japan

<sup>a)</sup>Authors to whom correspondence should be addressed: [maxime.giteau.pro@gmail.com](mailto:maxime.giteau.pro@gmail.com) and [jf.guillemoles@cnrs.fr](mailto:jf.guillemoles@cnrs.fr)

## ABSTRACT

Conventional single-junction solar cells have a theoretical efficiency limit around 33%, and multi-junction solar cells (MJSCs) are currently the only technology to overcome this limit. The demonstration of hot-carrier solar cells (HCSCs), another high-efficiency approach that relies on harvesting the kinetic energy of the photo-generated carriers, has so far been hindered due to the difficulty of mitigating carriers' thermalization. In this letter, we highlight the synergies of these two concepts by introducing the hot-carrier multi-junction solar cell (HCMJSC), a MJSC with a thin hot-carrier top junction. Using a detailed balance model, we compare the efficiency of different devices as a function of three parameters: the bandgap of the top and bottom junctions, the top cell thickness, and an effective thermalization coefficient, which encapsulates information on both thermalization and light trapping. Besides allowing for a much broader range of material combinations than MJSCs, we show that HCMJSCs can reach efficiencies higher than MJSCs with a larger thermalization coefficient than HCSCs. As such, HCMJSCs could provide a preferred route toward the development of hot-carrier-based high efficiency devices.

Published under an exclusive license by AIP Publishing. <https://doi.org/10.1063/5.0073274>

Single-junction solar cells are getting ever closer to the Shockley-Queisser (SQ) efficiency limit (around 33% under 1-sun illumination<sup>1</sup>). Only III-V Multi-Junction Solar Cells (MJSCs) have overcome the SQ limit so far, with a record efficiency of 47.1% under concentrated sunlight for a six-junction cell.<sup>2,3</sup> Achieving such high efficiencies with two-terminal devices (which are favored since they are much easier to integrate in a photovoltaic installation) requires perfect current-matching between the junctions, i.e., a constrained combination of bandgaps for each subcell. One challenge is, therefore, to find materials with the proper combination of bandgaps that can be stacked together. This has been the subject of many successful technological developments, most of them addressing the epitaxial lattice-matching constraints in single-crystal semiconductors.<sup>3-8</sup> Still, the efficiency gain becomes smaller and smaller as the number of junctions increases, while the device becomes more costly as well as more sensitive to spectral variations.<sup>9</sup> In this context, alternative technologies are being explored to achieve ultimate efficiencies.

The Hot-Carrier Solar Cell (HCSC) is another photovoltaic concept with the same theoretical limit as infinite-junctions MJSCs (around 85% under full concentration<sup>10</sup>) but for a single-junction device. This

concept relies on extracting carriers at a higher temperature than the lattice by preventing thermalization, i.e., the energy-dissipating interactions between the carriers and the lattice. One obstacle for this technology is that the thermalization rate in conventional materials is too fast to achieve hot-carrier populations, even under concentrated sunlight illumination. Ultrathin absorbers, in particular, those with quantized energy levels, exhibit a significantly lower thermalization rate,<sup>11-15</sup> and have led to the development of promising proofs of concept.<sup>16</sup> However, such ultrathin absorbers cannot absorb efficiently low-energy photons close to the bandgap, resulting in a low current limiting the efficiency. One way to combine a slow thermalization rate with strong light absorption is the combination of ultrathin absorbers with broadband light trapping.<sup>17</sup> Still, there are theoretical limits to how much light trapping can be achieved,<sup>18-20</sup> and current implementations remain far below these limits.<sup>21</sup> Thus, achieving broadband absorption enhancements compatible with HCSC operation is an overlooked major challenge for this technology.

Here, we propose a way to achieve strong hot-carrier effects in ultrathin absorbers while still absorbing most photons, even without light trapping, by combining the advantages of HCSCs and MJSCs.

High-energy photons, which contribute the most to the generation of a hot-carrier population,<sup>15</sup> are typically absorbed within a few tens of nanometers. By contrast, photons with an energy close to the bandgap require much thicker absorbers while not contributing significantly to hot-carrier generation. Therefore, although these low-energy photons must be absorbed to reach high currents and ultimately high efficiencies, they do not need to be absorbed in the hot-carrier absorber. In this Letter, we propose a device architecture, which we call Hot-Carrier Multi-Junction Solar Cell (HCMJSC), where a thin hot-carrier top junction absorbs high-energy photons while low-energy photons are absorbed in a second, thicker junction.

The absorption profile of the HCSC, MJSC, and HCMJSC is compared in Fig. 1. In the thin HCSC [Fig. 1(a)], photons cannot be absorbed effectively, while in the HCMJSC [Fig. 1(b)], the photons not absorbed in the hot-carrier junction are collected in a second junction. As a result, the photons with intermediate energy are distributed between both junctions. This differs from an ideal MJSC where each subcell absorbs a specific spectral bandwidth [Fig. 1(c)]. In the absence of hot-carrier effects, the multi-junction solar cell will offer the highest efficiency limit. However, as the thermalization is reduced in the top cell, both the HCSC and the HCMJSC will gain in efficiency. Studying the impact of absorber thickness, bandgap, and thermalization rate on the efficiency of HCSC, MJSC, and HCMJSC devices, we show in the following that the HCMJSC can achieve the highest efficiencies for intermediate values of thermalization while lifting design constraints.

The system is modelled using a detailed balance formalism,<sup>1,22</sup> with ideal assumptions regarding carrier collection and radiative efficiency for both junctions (considering a constant radiative to non-radiative recombination rate as in Ref. 1, we verified that non-radiative recombination degrades all devices in a comparable fashion). The model considers a balance equation for the current,  $J_{abs} = J_{rad} + J_{ext}$ , where  $J_{abs}$  is the photocurrent,  $J_{rad}$  is the radiatively recombined current, and  $J_{ext}$  is the current extracted from the system. Hot-carrier effects are included (only in the top junction) by introducing a balance equation for the power:<sup>10,23</sup>  $P_{abs} = P_{rad} + P_{ext} + P_{th}$ , where  $P_{abs}$ ,  $P_{rad}$ , and  $P_{ext}$  are the power quantities for the currents described above, and  $P_{th}$  is the power lost in carrier cooling (intraband thermalization). We

also assume carriers are extracted isentropically through selective contacts where they cool while their chemical potential increases,<sup>10,17</sup> a process akin to the thermoelectric effect.

To model tandem junctions, the detailed balance equations are solved for each sub-junction separately. A current-match constraint is then applied to determine the efficiency of the device. (We neglect potential losses in the tunnel junction.) Since the absorber thickness plays a critical role on both absorption and thermalization, we consider models (described below) that take into account that thickness dependence in order to compare the different devices.

Previous works have found a linear relationship between the thermalized power and the temperature difference between the carriers and the lattice.<sup>15,24–26</sup> Furthermore, we have shown recently that thermalization in bulk absorbers can be divided into interface and volume contributions, the second being attributable to electron-phonon interactions within the absorber.<sup>15</sup> Assuming negligible contribution from the interface (whose origin remains to be understood), the thermalization strength is proportional to the thickness of the device and the thermalized power can be described semi-empirically as

$$P_{th} = q_V d (T_c - T_L), \quad (1)$$

where  $q_V$  is the volume thermalization coefficient of the absorber,  $d$  is its thickness, and  $T_c$  and  $T_L$  are the temperature of the carriers and of the lattice, respectively. Here,  $q_V$  is treated as a variable parameter of the model.

The absorptivity  $A$  is modeled with a simple Beer-Lambert law, accounting for light trapping by introducing a wavelength-independent light path enhancement<sup>17</sup>  $F$ , such that

$$A(\lambda) = 1 - \exp(-F\alpha(\lambda)d), \quad (2)$$

where  $\lambda$  is the photon wavelength and  $\alpha$  is the absorption coefficient.  $F \times d$  is the optical thickness of the device. This absorption allows to calculate the photocurrent  $J_{abs} = q \cdot \int A(\lambda) \Phi_{sun}(\lambda) d\lambda$  (where  $q$  is the elementary charge and  $\Phi_{sun}$  is the photon flux incident from the sun), as well as the radiative recombination  $J_{rad}$  given by the generalized Planck law.<sup>17,27</sup> We take into account the band filling dependence of the absorption coefficient,<sup>16,17</sup> which is necessary to accurately

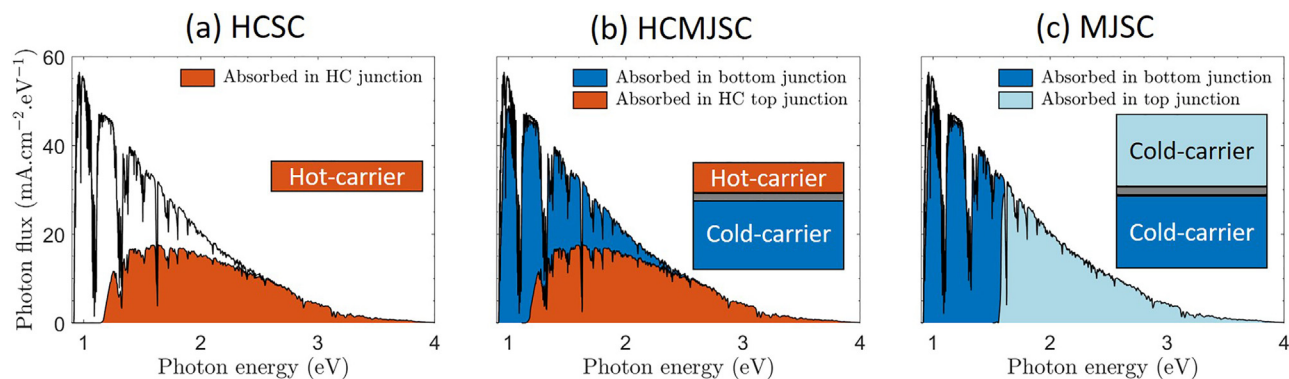


**FIG. 1.** Absorbed fraction of the incident photon flux (AM1.5D spectrum) as a function of the photon energy for: (a) A HCSC with a thin absorber ( $d = 200$  nm,  $E_G = 1.19$  eV). (b) The HCMJSC concept presented in this Letter, with a thin hot-carrier junction ( $d = 200$  nm,  $E_G = 1.19$  eV) on top of a thick bottom junction ( $d = 2$   $\mu$ m,  $E_G = 0.93$  eV). The photons not absorbed in the hot-carrier top junction are collected in the bottom junction. (c) A MJSC made with a thick top ( $d = 2$   $\mu$ m,  $E_G = 1.59$  eV) and thick bottom ( $d = 2$   $\mu$ m,  $E_G = 0.93$  eV) absorbers. Unlike for HCMJSC, the spectrum is sharply divided between both junctions. The absorption coefficients considered here are obtained by extrapolation from the absorption coefficients of InP ( $E_G = 1.344$  eV) and InGaAs ( $E_G = 0.74$  eV).

estimate the radiated current and power, especially under concentrated illumination.

Within this model,  $q_V$  and  $F$  play a similar role on the efficiency of the device. Indeed, reducing the thickness  $d$  of the device while keeping its optical thickness  $F \times d$  constant (through increased light trapping) only affects the thermalized power  $P_{th}$  in the detailed balance equations. It is, therefore, equivalent to reducing the thermalization coefficient  $q_V$  while keeping both  $d$  and  $F$  constant.<sup>17,28</sup> As a result, the effective volume thermalization coefficient  $q_V/F$  can be varied as a single parameter to assess the efficiency of a device with a given optical thickness.

In order to study the influence of the bandgap combination on the efficiency of the device, we need a realistic description of the wavelength-dependent absorption coefficient  $\alpha(\lambda)$  as a function of the bandgap. To do so, we extrapolate linearly the refractive index between InGaAs<sup>29</sup> ( $E_G = 0.74$  eV) and InP<sup>30</sup> ( $E_G = 1.344$  eV) to bandgaps between 0.6 and 1.8 eV. The procedure is illustrated in the [supplementary material](#), Fig. S1.

For tandem junctions, the optical thickness of the bottom cell is fixed to  $2 \mu\text{m}$ , and the optical thickness of the top cell is constrained to ensure current matching at maximum power point. (If current matching cannot be achieved, the optical thickness is fixed to  $2 \mu\text{m}$ .) For the HCSC, we consider an optical thickness of  $2 \mu\text{m}$  to ensure good absorption. We consider a concentration of 1000 suns (AM1.5D spectrum), which is the order of magnitude of current high-concentration photovoltaic systems. Within this framework, the efficiency of each device is a function of at most three independent parameters: the bandgaps of the junctions and the effective thermalization coefficient  $q_V/F$ .

We consider the optimal tandem solar cell as a reference device. With our model, we find a maximum MJSC efficiency  $\eta = 53.15\%$ , obtained for  $E_{G,top} = 1.59$  eV and  $E_{G,bot} = 0.93$  eV, with a thick top junction ( $2 \mu\text{m}$ ). These values are close to those obtained from a detailed balance model considering step absorption.<sup>31</sup> Importantly, this combination of bandgaps cannot be obtained with a lattice-matched combination of conventional III-V materials.<sup>32</sup> To emphasize the realistic prospects of HCMJSCs, we restrict its bandgaps to those of InGaAsP compounds lattice-matched to InP ( $0.74 \text{ eV} \leq E_G \leq 1.344 \text{ eV}$ ). Irrespective of the bandgap of the top cell and of the effective thermalization coefficient  $q_V/F$ , we observe that the highest efficiency is always obtained for a bottom cell with a bandgap around  $E_{G,bot} = 0.93$  eV. (Small variations of this bandgap do not lead to significant departure from the optimum.) Therefore, we consider the same  $2 \mu\text{m}$ -thick bottom junction for both MJSC and HCMJSC. We compare the efficiency of both technologies for different HCMJSC top cell bandgaps as a function of  $q_V/F$  (see the [supplementary material](#), Fig. S2). As the thermalization coefficient becomes smaller, the HCMJSC becomes more efficient than the MJSC thanks to an increased hot-carrier effect. Furthermore, the HCMJSC device with a top InP cell ( $E_{G,top} = 1.344$  eV, the largest bandgap achievable given the material constraint) of effective thickness  $265 \text{ nm}$  and a bottom  $2 \mu\text{m}$ -thick InGaAsP cell of bandgap  $E_{G,bot} = 0.93$  eV offers the highest efficiency among all HCMJSCs for all thermalization coefficients, and surpasses the MJSC for  $q_V/F \leq 1000 \text{ W cm}^{-3} \text{ K}^{-1}$ . Crucially, the HCMJSC design leads to the reduction of the top junction's optical thickness by one order of magnitude compared to a conventional MJSC.

Now that we know that HCMJSCs can overcome ideal MJSCs, we compare the optimal HCMJSC device just identified with HCSCs

of different bandgaps as a function of  $q_V/F$  (see the [supplementary material](#), Fig. S3). For a low-enough thermalization, the HCSCs reach higher efficiencies than the HCMJSC, since they take better advantage of hot-carrier effects. Furthermore, the smaller the bandgap of the HCSC, the larger the  $q_V/F$  for which it overcomes the HCMJSC efficiency. The optimal HCSC on InP is, thus, an InGaAs cell with bandgap  $E_G = 0.74$  eV and an effective thickness of  $2 \mu\text{m}$ , which surpasses the HCMJSC for  $q_V/F \leq 50 \text{ W cm}^{-3} \text{ K}^{-1}$ .

To summarize, we compare the three optimal devices as a function of the effective thermalization coefficient  $q_V/F$ , leading to the identification of three regions (Fig. 2). For high thermalization, hot-carrier effects are small and the ideal MJSC offers the highest efficiency. When the thermalization is very low, the HCSC is preferable since it benefits fully from hot carriers. A key result of this paper is that HCMJSCs can be more efficient than both HCSCs and MJSCs for a large range of intermediate values of the effective thermalization coefficients ( $50 \leq q_V/F \leq 1000 \text{ W cm}^{-3} \text{ K}^{-1}$  for 1000 sun illumination). Furthermore, the HCSC reaches a higher efficiency than the MJSC only for  $q_V/F \leq 100 \text{ W cm}^{-3} \text{ K}^{-1}$ . The HCMJSC approach, thus, allows to relax the constraint on the effective thermalization coefficient by one order of magnitude, which is attributable to the order-of-magnitude reduction in the hot-carrier junction's optical thickness.

To put this result into perspective, the values of  $q_V/F$  identified here should be compared, for example, to the volume thermalization coefficient  $q_V \approx 2 \times 10^6 \text{ W cm}^{-3} \text{ K}^{-1}$  measured in bulk GaAs.<sup>15</sup> Even with optimistic broadband light trapping ( $F = 20$ ), this value of  $q_V$  is 3 orders of magnitude too high for HCSCs to be competitive with MJSCs. With the HCMJSC architecture, the gap remains significant although it is reduced to a factor 100. The main way to bridge this gap is through the development of low-thermalization absorbers, for example, quantum nanostructures made of materials with slower electron-phonon interactions than GaAs.<sup>16</sup> In that regard, HCMJSCs can implement nanostructured absorbers more

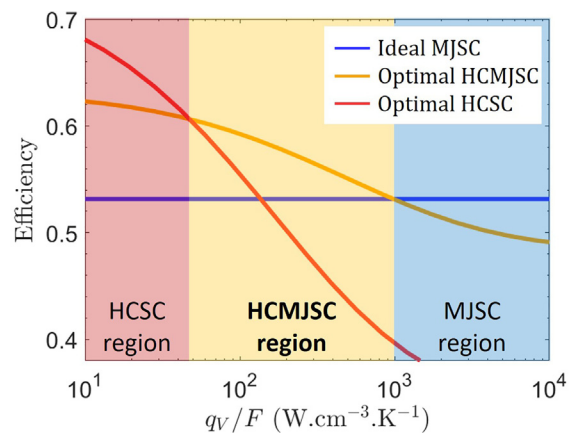


**FIG. 2.** Comparison of the efficiency of the ideal MJSC (blue line,  $E_{G,top} = 1.59$  eV and  $E_{G,bot} = 0.93$  eV), the optimal HCMJSC (yellow line,  $E_{G,top} = 1.344$  eV and  $E_{G,bot} = 0.93$  eV) and the optimal HCSC (red line,  $E_G = 0.74$  eV) as a function of the effective thermalization coefficient  $q_V/F$  for different bandgaps under 1000 sun illumination (AM1.5D spectrum). Three regions can be distinguished. The MJSC offers the highest efficiency for strong thermalization, while the HCSC is the most efficient at low thermalization. For intermediate values ( $50 \leq q_V/F \leq 1000 \text{ W cm}^{-3} \text{ K}^{-1}$ ), the HCMJSC outperforms the other two technologies.



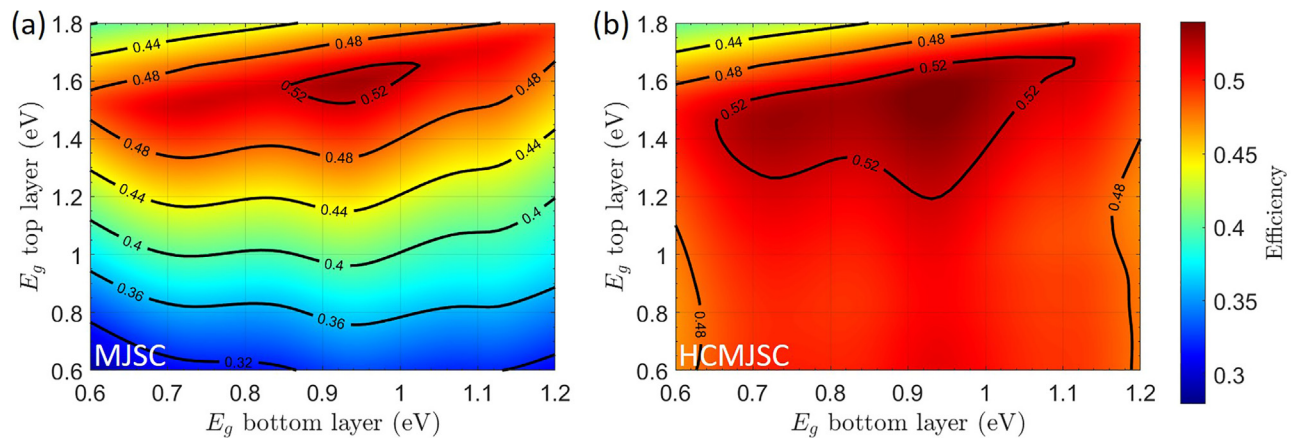


**FIG. 3.** Efficiency of a tandem device as a function of the bandgap of the top and bottom junctions, under 1000 sun illumination (AM1.5D spectrum). The absorption coefficients are extrapolated from InP and InGaAs lattice-matched to InP. The thickness of the bottom cell is  $2\ \mu\text{m}$  and that of the top cell is adjusted to ensure current matching (see the [supplementary material](#), Fig. S4). (a) The carriers are considered cold, and the efficiency is that of a classical tandem solar cell. (b) Hot carriers are considered in the top cell, with a volume thermalization coefficient  $q_V = 1000\ \text{W cm}^{-3}\ \text{K}^{-1}$ .

easily than HCSCs, as they require much smaller optical thicknesses. Still other parameters can help to tip the scales in favor of HCMJSCs, like increasing the concentration beyond 1000 suns or increasing the number of junctions (as this will reduce the optical thickness required for the top junction). It should nonetheless be noted that accounting for the non-ideality of the selective contacts in hot-carrier devices will reduce somewhat their efficiency relative to MJSCs. Overall, although this remains a significant challenge, the HCMJSC architecture makes it more feasible for hot-carrier devices to reach technological maturity, with real prospects to achieve efficiencies comparable to those of MJSCs.

Finally, we compare the influence of the bandgaps of the top and bottom junctions on the efficiency of MJSC and HCMJSC, for a fixed  $q_V/F = 1000\ \text{W cm}^{-3}\ \text{K}^{-1}$  (Fig. 3). This value was chosen as it corresponds to the efficiency crossing point for optimal devices (Fig. 2). Although the maximum efficiency of both devices is similar, the range of bandgaps over which the efficiency of HCMJSC is close to its maximum is much larger than for MJSC, especially regarding the top cell bandgap. Indeed, HCMJSCs with a narrower top-junction bandgap, although less effective as MJSCs, benefit more from hot-carrier effect, both because they are thinner and because they generate more kinetic power per absorbed photon (see [supplementary material](#) Fig. S4 for the top cell thickness corresponding to each bandgap combination). As a result, HCMJSCs offer a much larger range of acceptable bandgaps than MJSCs, relaxing the epitaxial growth requirements. In particular, tandem homojunctions, and even devices where the top bandgap is smaller than the bottom one ( $E_{G,\text{top}} \leq E_{G,\text{bot}}$ ), could achieve relatively high efficiencies in the HCMJSC configuration.

In conclusion, we have shown that the HCMJSC, which consists in a MJSC with a thin hot-carrier top junction, offers several advantages relative to both HCSCs and MJSCs. The most important one is that HCMJSCs can achieve efficiencies higher than MJSCs for an effective thermalization coefficient one order of magnitude higher than HCSCs, strongly improving the prospects of hot-carrier devices. As materials with slower thermalization rates are developed together with improved light trapping architectures and concentrator systems, we

believe that the HCMJSC has the potential to become the next generation of high efficiency solar cells, as well as the stepping stone toward single-junction HCSCs. Besides efficiency considerations, HCMJSCs offer the important advantage of showing high efficiencies for a large range of bandgap combinations compared to MJSCs. This opens up new material combinations, including devices with a lower-bandgap material for the top cell rather than for the bottom cell. Additionally, HCMJSCs require much thinner top cells than MJSCs, meaning lower fabrication costs thanks to a higher production throughput and material savings.

See the [supplementary material](#) for details on the interpolation of the absorption coefficient with bandgap as well as additional results on HCMJSCs.

The authors would like to acknowledge support from the LIA-NextPV Program between CNRS, France, and RCAST, the University of Tokyo, Japan, and thank Daniel Suchet for fruitful discussions. This research was supported by the French Government in the frame of the program of investment for the future (Programme d'Investissement d'Avenir—Grant No. ANR-IEED-002-01).

## AUTHOR DECLARATIONS

### Conflict of Interest

The authors have no conflicts of interest to declare.

### DATA AVAILABILITY

The data that support the findings of this study are available from the corresponding authors upon reasonable request.

## REFERENCES

- <sup>1</sup>W. Shockley and H. J. Queisser, *J. Appl. Phys.* **32**, 510 (1961).
- <sup>2</sup>M. A. Green, E. D. Dunlop, J. Hohl-Ebinger, M. Yoshita, N. Kopidakis, and X. Hao, *Prog. Photovoltaics: Res. Appl.* **29**, 657 (2021).
- <sup>3</sup>J. F. Geisz, R. M. France, K. L. Schulte, M. A. Steiner, A. G. Norman, H. L. Guthrey, M. R. Young, T. Song, and T. Moriarty, *Nat. Energy* **5**, 326 (2020).

- <sup>4</sup>M. Wanlass, P. Ahrenkiel, D. Albin, J. Carapella, A. Duda, K. Emery, D. Friedman, J. Geisz, K. Jones, A. Kibbler, J. Kiehl, S. Kurtz, W. McMahon, T. Moriarty, J. Olson, A. Ptak, M. Romero, and S. Ward, in *IEEE 4th World Conference on Photovoltaic Energy Conference* (IEEE, 2006), Vol. 1, pp. 729–732.
- <sup>5</sup>S. R. Kurtz, A. A. Allerman, E. D. Jones, J. M. Gee, J. J. Banas, and B. E. Hammons, *Appl. Phys. Lett.* **74**, 729 (1999).
- <sup>6</sup>M. Wiemer, V. Sabnis, and H. Yuen, in *High and Low Concentrator Systems for Solar Electric Applications VI* (International Society for Optics and Photonics, 2011), Vol. 8108, p. 810804.
- <sup>7</sup>F. Dimroth, M. Grave, P. Beutel, U. Fiedeler, C. Karcher, T. N. D. Tibbits, E. Oliva, G. Siefer, M. Schachtner, A. Wekkeli, A. W. Bett, R. Krause, M. Piccin, N. Blanc, C. Drazek, E. Guiot, B. Ghyselen, T. Salvetat, A. Tauzin, T. Signamarcheix, A. Dobrich, T. Hannappel, and K. Schwarzbürg, *Prog. Photovoltaics* **22**, 277 (2014).
- <sup>8</sup>A. Freundlich and A. Alemu, *Phys. Status Solidi C* **2**, 2978 (2005).
- <sup>9</sup>P. Faine, S. R. Kurtz, C. Riordan, and J. M. Olson, *Solar Cells* **31**, 259 (1991).
- <sup>10</sup>R. T. Ross and A. J. Nozik, *J. Appl. Phys.* **53**, 3813 (1982).
- <sup>11</sup>W. S. Pelouch, R. J. Ellingson, P. E. Powers, C. L. Tang, D. M. Szmyd, and A. J. Nozik, *Phys. Rev. B* **45**, 1450 (1992).
- <sup>12</sup>Y. Rosenwaks, M. C. Hanna, D. H. Levi, D. M. Szmyd, R. K. Ahrenkiel, and A. J. Nozik, *Phys. Rev. B* **48**, 14675 (1993).
- <sup>13</sup>L. C. Hirst, M. K. Yakes, C. G. Bailey, J. G. Tischler, M. P. Lumb, M. González, M. F. Führer, N. J. Ekins-Daukes, and R. J. Walters, *IEEE J. Photovoltaics* **4**, 1526 (2014).
- <sup>14</sup>G. Conibeer, Y. Zhang, S. P. Bremner, and S. Shrestha, *Jpn. J. Appl. Phys., Part 1* **56**, 091201 (2017).
- <sup>15</sup>M. Giteau, E. de Moustier, D. Suchet, H. Esmailpour, H. Sodabanlu, K. Watanabe, S. Collin, J.-F. Guillemoles, and Y. Okada, *J. Appl. Phys.* **128**, 193102 (2020).
- <sup>16</sup>D.-T. Nguyen, L. Lombez, F. Gibelli, S. Boyer-Richard, A. Le Corre, O. Durand, and J.-F. Guillemoles, *Nat. Energy* **3**, 236 (2018).
- <sup>17</sup>M. Giteau, D. Suchet, S. Collin, J.-F. Guillemoles, and Y. Okada, *EPJ Photovoltaics* **10**, 1 (2019).
- <sup>18</sup>E. Yablonovitch, *J. Opt. Soc. Am.* **72**, 899 (1982).
- <sup>19</sup>Z. Yu, A. Raman, and S. Fan, *Proc. Natl. Acad. Sci.* **107**, 17491 (2010).
- <sup>20</sup>S. Collin and M. Giteau, in *IEEE 7th World Conference on Photovoltaic Energy Conversion (WCPEC) (A Joint Conference of 45th IEEE PVSC, 28th PVSEC 34th EU PVSEC)* (IEEE, 2018), pp. 3460–3462.
- <sup>21</sup>I. Massiot, A. Cattoni, and S. Collin, *Nat. Energy* **5**, 959 (2020).
- <sup>22</sup>J. Guillemoles, T. Kirchartz, D. Cahen, and U. Rau, *Nat. Photonics* **13**, 501 (2019).
- <sup>23</sup>A. L. Bris, J. Rodiere, C. Colin, S. Collin, J. L. Pelouard, R. Esteban, M. Laroche, J. J. Greffet, and J. F. Guillemoles, *IEEE J. Photovoltaics* **2**, 506 (2012).
- <sup>24</sup>A. L. Bris, L. Lombez, S. Laribi, G. Boissier, P. Christol, and J.-F. Guillemoles, *Energy Environ. Sci.* **5**, 6225 (2012).
- <sup>25</sup>L. C. Hirst, H. Fujii, Y. Wang, M. Sugiyama, and N. J. Ekins-Daukes, *IEEE J. Photovoltaics* **4**, 244 (2014).
- <sup>26</sup>H. Esmailpour, B. K. Durant, K. R. Dorman, V. R. Whiteside, J. Garg, T. D. Mishima, M. B. Santos, I. R. Sellers, J.-F. Guillemoles, and D. Suchet, *Appl. Phys. Lett.* **118**, 213902 (2021).
- <sup>27</sup>P. Würfel, *J. Phys. C* **15**, 3967 (1982).
- <sup>28</sup>M. Giteau, K. Watanabe, N. Miyashita, H. Sodabanlu, J. Goffard, A. Delamarre, D. Suchet, R. Tamaki, Z. Jehl, L. Lombez, M. Sugiyama, A. Cattoni, S. Collin, J.-F. Guillemoles, and Y. Okada, *Physics, Simulation, and Photonic Engineering of Photovoltaic Devices VIII* (International Society for Optics and Photonics, 2019), Vol. 10913, p. 109130D.
- <sup>29</sup>S. Adachi, *J. Appl. Phys.* **66**, 6030 (1989).
- <sup>30</sup>*Handbook of Optical Constants of Solids*, edited by E. D. Palik (Academic Press, 1998).
- <sup>31</sup>D. J. Friedman, *Curr. Opin. Solid State Mater. Sci.* **14**, 131 (2010).
- <sup>32</sup>A. Bett, F. Dimroth, G. Stollwerck, and O. Sulima, *Appl. Phys. A* **69**, 119 (1999).